Published in final edited form as:
Eur J Neurosci. 2009 April ; 29(7): 1408–1421. doi:10.1111/j.1460-9568.2009.06693.x.

The maintenance of specific aspects of neuronal function and behavior is dependent on programmed cell death of adult-generated neurons in the dentate gyrus

Woon Ryoung Kim[1], **Ok-hee Park**[1], **Sukwoo Choi**[3], **Se-Young Choi**[4], **Soon Kwon Park**[1], **Kea Joo Lee**[1], **Im Joo Rhyu**[1], **Hyun Kim**[1], **Yeon Kyung Lee**[2], **Hyun Taek Kim**[2], **Ronald W Oppenheim**[5], and **Woong Sun**[1,*]

[1] Department of Anatomy, Korea University College of Medicine, Brain Korea 21

[2] Department of Psychology, Korea University

[3] Division of Biological Sciences, Seoul National University

[4] School of Dentistry, Seoul National University

[5] Department of Neurobiology and Anatomy and Neuroscience Program, Wake Forest University School of Medicine, Winston-Salem, North Carolina 27157

Abstract

A considerable number of new neurons are generated daily in the dentate gyrus (DG) of the adult hippocampus, but only a subset of these survive, as many adult-generated neurons undergo programmed cell death (PCD). However, the significance of PCD in the adult brain for the functionality of DG circuits is not known. Here we examined the electrophysiological and behavioral characteristics of Bax-KO mice in which PCD of post-mitotic neurons is prevented. The continuous increase in DG cell numbers in Bax-KO mice, resulted in the readjustment of afferent and efferent synaptic connections, represented by age-dependent reductions in the dendritic arborization of DG neurons and in the synaptic contact ratio of mossy fibers (MF) with CA3 dendritic spines. These neuroanatomical changes were associated with reductions in synaptic transmission and reduced performance in a contextual fear memory task in 6-month old Bax-KO mice. These results suggest that the elimination of excess DG neurons via Bax-dependent PCD in the adult brain is required for the normal organization and function of the hippocampus.

Keywords

cell death; Bax; adult neurogenesis; LTP; synapse

Introduction

The elimination of unnecessary neuronal connections is essential for the establishment and maintenance of efficient synaptic function. Two major developmental strategies are available for this process, programmed cell death (PCD) and synapse elimination (Buss et al., 2006a). Neuronal PCD is involved in the optimal quantitative matching of neurons in a population with available synaptic targets (systems-matching) (Hamburger and Oppenheim, 1982). PCD in this context is thought to be regulated by competition among innervating

*Correspondence should be addressed to Woong Sun, Ph.D, Department of Anatomy, Brain Korea 21, Korea University College of Medicine, Anam-Dong, Sungbuk-Gu, Seoul, Korea 136-705, Tel: +02-920-6404; Fax: +02-929-5696, woongsun@korea.ac.kr.

neurons for limited amounts of target-derived trophic signals (Buss et al., 2006a; Oppenheim, 1991; Purves, 1988). From this perspective, it is surprising that despite the complete prevention of PCD by deletion of the pro-apoptotic gene Bax, the structure and function of the nervous system is reported to be relatively normal (Buss et al., 2006b; Sun et al., 2004). This appears to be partly explained by the observation that many of the rescued neurons in Bax-KO mice fail to maintain synaptic connections with their targets (Sun et al., 2003) resulting in quantitative systems-matching that is comparable to control mice. Despite the absence of PCD other compensatory mechanisms such as synapse elimination are able to perform a systems-matching function indicating that PCD in this situation is not required.

Following the major period of developmental neurogenesis, a substantial number of new neurons continue to be added to the dentate gyrus (DG) of the adult brain throughout life in many species, including humans (Altman & Das, 1965; Caviness, 1973; Kaplan & Hinds, 1977; Eriksson et al., 1998). And similar to the situation during development, substantial numbers (30–70%) of newly generated DG immature neurons in the adult brain undergo PCD (Cameron & McKay, 2001; Dayer et al., 2003; Sun et al., 2004). The PCD of relatively mature DG neurons has been reported in the rodent hippocampus (Dayer et al., 2003), although the extent of this type of PCD and its significance as a cell renewal/turnover process are issues still being debated (Gross, 2000; Wiskott et al., 2006; Ninkovic et al., 2007). It has been proposed that adult neurogenesis and hippocampal function, including learning and memory are closely related (Kempermann et al., 1997; Gould et al., 1999; van Praag et al., 1999). For instance, prevention of adult neurogenesis by either irradiation or selective elimination of adult-produced DG neurons by the use of an inducible genetic strategy consistently impairs hippocampus-dependent associative learning (Saxe et al., 2006; Imayoshi et al., 2008) and mutant animals with impaired adult neurogenesis also exhibit alterations in hippocampus-related behaviors (Feng et al., 2001; Cao et al., 2004; Saxe et al., 2006; Denis-Donini et al., 2008; Dupret et al., 2007; Zhang et al., 2008). Learning of hippocampus-dependent tasks enhances the survival of adult generated neurons, suggesting that PCD may be an essential regulatory step in the activity- or experience-related function of adult neurogenesis. However, there are also contrasting results demonstrating the dissociation of learning and adult neurogenesis, indicating that the precise relationship between adult neurogenesis and learning remains to be elucidated (Leuner et al., 2004).

Recently we demonstrated that the PCD of adult-produced DG neurons is dependent on the pro-apoptotic gene Bax, and that genetic elimination of Bax rescues virtually all adult-produced DG neurons from death resulting in an age-dependent accumulation of DG neurons (Sun et al., 2004). We have now extended these observations in the present study by demonstrating that these Bax-KO-rescued, adult-produced DG neurons appear to maintain synaptic contacts with afferent and efferent neurons, which perturbs systems-matching and alters some aspects of normal hippocampal function.

Materials and Methods

Animals

Bax-KO mice were purchased from Jackson Lab (Bar harbor, ME). Mice were maintained on a C57BL/6 background after being backcrossed for >10 generations with C57BL/6 mice. Homozygous Bax-defiecient (Bax-KO) and WT littermate mice were generated from matings between heterozygous males and females. Sibling animals were collected individually and genotyped by PCR (Knudson et al., 1995). All experiments were carried out in accordance with the regulations and approval of the Animal Care and Use Committee of the Korea University.

Electrophysiology

After cervical dislocation, mouse brains were removed quickly and chilled in ice-cold oxygenated cutting buffer (175 mM sucrose, 20 mM NaCl, 3.5 mM KCl, 1.25 mM NaH_2PO_4, 25.6 mM $NaHCO_3$, 1.3 mM $MgCl_2$, 10 mM D-(+)-glucose). Transverse hippocampus slices (400 μm) were cut using a Vibratome. The slices were then transferred to a recording chamber containing oxygenated artificial cerebrospinal fluid (ACSF; 120 mM NaCl, 3.5 mM KCl, 1.25 mM NaH_2PO_4, 25.6 mM $NaHCO_3$, 1.3 mM $MgCl_2$, 10 mM D-(+)-glucose, 2 mM $CaCl_2$) and allowed to recover at RT for at least 30 min before recording (Schmitz et al., 2003). During the recording, slices were maintained in a recording chamber with a 3–4 ml/min perfusion rate. To record synaptic responses, a concentric tungsten bipolar stimulating electrode (100 μm in diameter; Rhodes Medical Supply) was used for stimulation and a high-resistance recording electrode (1- to 2-μm tip) filled with 0.9% NaCl was used for field recording. Extracellular field potentials were amplified using a DP-301 amplifier (Warner Instrument Co., Hamden, CT) and the output was digitized with a DIGIDATA 1322A interface (Molecular Devices, Union City, CA). The digitized signals were stored and analyzed with a PC computer using pClamp 8 (Axon Instruments Inc., Foster City, CA). Electrophysiological recordings were carried out as follows:

Mossy fiber (MF) circuits—For MF LTP (as shown in the inset of Figure 5B), the field potential recordings were obtained in the stratum lucidum of CA3 following stimulation of the polymorph layer near the upper blade of DG. Input-output curves were plotted with synaptic responses (field excitatory postsynapytic potential, fEPSP) against presynaptic fiber volley amplitude. Pulses paired with varying interpulse intervals (40, 80, 120 and 240 ms) were applied at a repetition rate of 0.0083Hz. Each data point is an average of two measurements per slice. For the measurement of long term potentiation (LTP), synaptic responses were elicited at 0.017 Hz. The stimulation intensity that produced a half-maximal response (50–90 μA, 5–9 msec peak latency) was chosen for test pulse and tetanic stimulation. Only those slices which produced a fEPSP of 0.4 mV or higher in amplitude were included in the analysis. Baseline was then taken for 30 min, and MF LTP was induced by 4 trains of 100 Hz for 1 sec with 30 sec intervals. The fEPSP was recorded for 60-min periods. To confirm that fEPSPs were elicited by activation of monosynaptic fibers, 2 μM DCG-IV (Tocris, Ellisville, MO), a metabotropic glutamate receptor agonist, was applied at the end of the experiment as previously described (Schmitz et al., 2003). Results were included only if the remaining responses were less than 20%. The same experimental procedures were employed for all age groups of WT and Bax-KO mice.

Medial perforant pathway (mPP)—The field potential was recorded in the granule cell layer of the DG following stimulation of the molecular layer. For LTP measurements, synaptic responses were elicited at 0.017 Hz. The stimulationintensity that produced a half-maximal response (30–60 μA, 6–9 msec peak latency) was chosen for test pulse and tetanic stimulation. Only those slices which produced fEPSPs of 0.5 mV or higher in amplitude and paired-pulse depression were included in the analysis. Baseline was then taken for 30 min, followed by high frequency stimulation (HFS, 4 trains of 100 Hz for 1 sec with 30 sec intervals) using the same intensity and pulse duration as the test stimuli and further testing continued forat least 60 min. LTP induction rate was assessed as the mean of fEPSP amplitude for the last 30 min. In some experiments, mPP LTP was induced in the presence of picrotoxin in the bath solution (ACSF) which we refer to as picrotoxin-LTP. For picrotoxin-LTP, picrotoxin (50 μM, Sigma, St. Louis, MO) was applied to the perfusate 30 min prior to the recording (Snyder et al., 2001; Saxe et al., 2006).

Timm's staining

Mice were perfused with fixative containing 0.1% NaS, 4% paraformaldehyde and 1% glutaraldehyde in Tris-buffered saline (pH 7.4). Following frozen sectioning (40 μm), sections were submerged in a dense solution of 60 parts of arabic gum (diluted 1:2 in distillated water), 30 parts of hydroquinone (diluted 5.67 mg/100 ml in distillated water), 1 part silver nitrate (170 mg/ml indistillated water) and 9 parts citrate buffer (12.75 mg of $C_6H_8O_7$ and 11.75 mg of $C_6H_5O_7Na_3$ in 50 ml of distilled water, pH 4.0) for 1 hr (Ramirez-Amaya et al., 2001). After mounting, the silver-stained region of the hippocampus was measured in every 6th section spanning the entire hippocampus using Scion image software (NIH) and the sum of the total measures was considered as an individual value. Similarly, the area of the granule cell layer of the DG was obtained from adjacent sections after Nissl staining.

Immunohistochemistry

For calretinin labeling, animals were perfused with 4% paraformaldehyde and the brains were post-fixed in the same fixative for 24 hr. Brains were then cryoprotected in 30% sucrose, sectioned serially (40 μm) and subsequent immunostaining was performed by the free-floating method. For fluorescent-immunolabeling, anti-calretinin (Swant, Bellinzona, Switzerland, 1:1,000); anti-NeuN (Calbiochem, La Jolla, CA, 1:10,000); anti-activated caspase-3 (Cell signaling, Beverly, MA, 1:500) antibodies were applied overnight. After several washes with PBS, appropriate secondary antibodies were applied for 30 min. Subsequently, sections were washed, mounted and observed with a fluorescence or confocal microscope (Zeiss LSM510, Goetingen, Germany).

For bromodeoxyuridine (BrdU) labeling, mice were injected once intraperitoneally with a BrdU solution on P3 (50 μg/g body weight) after which the animals were killed 1-month following the injection. To quantify the number of BrdU labeled cells, every 12th section was pre-treated with 0.2 N HCl for 1 hr at 37°C. BrdU antibody (Roche Diagnostics, Mannheim, Germany, 1:10,000) was applied overnight. After several washes with PBS, a biotinylated horse anti-rat IgG (Vector Laboratories, Burlingame, CA, 1:500) secondary antibody was used, and labeling was visualized by avidin–biotinylated horseradish peroxidase complex Kit (ABC, Vector Laboratories, Burlingame, CA). Sections were mounted on gelatin-coated glass slides and air-dried. All sections were finally dehydrated in graded alcohols, cleared in xylene, and coverslipped with permount. After outlining of the DG layer with 10X magnification using a Zeiss Axio imager.A1 microscope (Goettingen, Germany), BrdU labeled cells in randomly selected areas (>20 area, 35×35 μm counting frame, 25 μm dissector height) under 40X magnification were counted by a computerized optical fractionator (Stereo Investigator software ver.7, mbf Bioscience, Williston, VT).

Golgi staining

Mice were anesthetized with an overdose of sodium pentobarbitol and perfused intracardially with 4% paraformaldehyde in 0.1 M Millonig's buffer. Tissue blocks (3 mm) were quickly dissected and coronal slices of hippocampus were further fixed in the same fixative overnight at 4°C. After washing with 0.1 N cacodylate buffer for 10 min, tissues were placed in 2.25% potassium dichromate and 0.4% osmium tetroxide for 3 days at 16–20° C in the dark. After a rinse with DW, tissues were further immersed in 0.75% $AgNO_3$ solution for 3 days in the dark. When staining was completed, the tissues were dehydrated and embedded in Epon-araldite mixture. The tissue blocks were serially sectioned in the coronal plane at 100 microns. Granule cells (20 cells per animal, n=5) whose cell bodies were localized in the granule cell layer (GCL) and that had continuous dendritic branches were sampled from the upper blade of the DG (Greenough et al., 1999). A two dimensional drawing of each neuron was traced using a camera-lucida microscope (Dialux 20EB, Leitz,

Germany), and the number of spines per unit length (10 μm) of dendrites that were located between 50–110 μm from the soma was counted. In addition, the number of dendritic branches at 80–90 μm from the soma was obtained as a measure of dendritic arborization. These data were plotted by cumulative frequency, and the statistical significance of the difference distribution was evaluated by Chi-square analysis.

Electron Microscopy

Preparation for transmission electron microscopy was performed based on previously published methods (Rhyu et al., 1999). Mice were anesthetized with sodium pentobarbital (100 mg/kg) and perfused with 2% paraformaldehyde/2.5% glutaraldehyde in 0.1 M phosphate buffer (pH 7.4). Coronal sections of the brains (0.4 mm) were washed, post-fixed in 2% osmium tetroxide for 2 hr, and *en bloc* stained with a uranyl acetate coloration solution for 90 min. The samples were then dehydrated through an ascending series of ethanol, propylene oxide, and embedded in Epon-Araldite mixture. Semi-thin sections cut in the CA3 dendritic fields were identified using the light microscope. Thin sections (70 nm) were made with a Reichert Ultracut, mounted on 200 mesh copper grids, stained with uranyl acetate followed by lead citrate. Electron micrographs were obtained using a Hitachi H-7500 (Hitachi, Tokyo, Japan) at the accelerating voltage of 80 kV. In each animal, approximately 60–70 images (20,000 x) were taken of proximal dendritic regions of CA3 pyramidal cells located in the upper border of the stratum pyramidale. The number of MF boutons, the size of MF boutons, and the ratio of synaptic contacts were determined from each single electron microscopy image, and the mean value from each animal was obtained. Because we did not obtain the MF volume from a 3-demensional reconstruction, the measurements represent only relative values for comparison. Only MF boutons with densely packed vesicles and dendritic spines with clear postsynaptic densities were included in the structural analyses. In addition, the number of spines on a single MF bouton and the size of individual MF boutons were obtained using Scion image Beta 4.02 (Scion Corp; Fredrick, MD).

Fear Conditioning

A Plexiglas shock chamber (24×24×24 cm) with a stainless-steel rod floor was used for training. Mice were placed in the chamber and allowed to habituate for 10 min and received 5 consecutive tone-conditioned stimuli (CS: 30 sec, 80 dB tone). Although pre-exposure to the CS is not essential for associative learning, this procedure is known to reduce unnecessary fear response to the (novel) conditioning context (Debiec et al., 2006; Doyère et al., 2007). On the next day, the unconditioned stimulus (US: 0.5 mA, 2 sec, scrambled footshock) was applied during the last 2 sec of the CS. Mice were given 2, 5, or 10 pairings to obtain ≥70% freezing behavior with 60±10 sec intertrial interval. After another 30 sec, the mice were returned to their home cage. Two hours after fear conditioning, mice were placed in the conditioning chamber without the CS for a period of 3 min for assessing contextual memory. The next day, the contextual memory test was performed using the same set of animals. In a pilot study, we found that possible extinction by the successive exposure of the animals did not substantially modify the results (data not shown). Three hr after the last 24-hr context fear test, mice were placed in a novel chamber for 2 min, and the CS tone was applied 3 times for assessing cued memory. Finally, 3 hr later mice were re-exposed to the conditioned chamber with CS tone for 2 min (cued+context test). Freezing responses were scored by the use of an automated system (SmartEye, ver.1.0).

Statistical analysis

Statistically significance differences between groups was evaluated by 2-tailed (α=0.05) one-way ANOVA (for the area measurements of the mossy fiber and of the granule cell layer of DG and PPF), with Scheffe's multiple comparison; Chi-square tests (for MF:CA3 synapses, MF bouton size frequency-fractionation and Golgi analysis); and independent

sample t-tests were also employed (other experiments). All the analyses were carried out with SPSS software (SPSS, Inc, Chicago, IL), and all values are given as mean ± SEM.

Results

Comparison of PCD in developmentally *vs.* adult produced hippocampal neurons

Previously we reported that the number of DG cells in wildtype (WT) and Bax-KO mice was similar in 2-month old animals but markedly increased in >6-month old animals, suggesting that the Bax-dependent PCD of DG neurons is critical in the adult brain *vs.* during early postnatal stages (Sun et al., 2004). Supporting this idea, we found that the extent of neuronal PCD in the E18-P15 WT DG is relatively low compared to the considerably greater cell death in the DG of 1–4 month-old WT mice (Fig. 1A–E). The extent of PCD was reduced between 6–12 months, which is consistent with the reported age-related reduction of neurogenesis (Kuhn et al., 1996; Ben Abdallah et al., 2008). Next, we labeled newly born neurons by a single BrdU injection on P3 and following a 1-month survival period, quantified the number of surviving BrdU-labeled neurons in the WT and Bax-KO DG (Fig. 1F–H). Because some cells exhibited a punctate pattern of BrdU-labeling, we separately counted both the dark BrdU-labeled cells and light (punctate) BrdU-labeled cells. In these comparisons, we found that the numbers of both dark and light BrdU-labeled, developmentally produced neurons were similar in WT and Bax-KO DG. Although sample size is relatively small, the low variance supports our interpretation that at these ages the PCD of new-born neurons is relatively low and that the number of $BrdU^+$ cells is similar in WT and Bax KO. This is in contrast to the substantially increased number of BrdU-labeled cells in Bax-KO mice (>3-fold increase compared to WT littermates) 1-month after a single BrdU injection in 2-month-old animals (Sun et al., 2004). Collectively, these results suggest that the PCD of developmentally produced DG neurons is relatively low, resulting in only a minor increase of DG neurons in young (1–2 month old) Bax-KO mice. Based on these observations we next examined the histological, electrophysiological, and behavioral characteristics of adult (6-month old) Bax-KO mice.

The morphological alteration of DG related circuits in Bax-KO mice

Because DG neuron number is selectively increased in adult *vs.* young Bax-KO mice, we examined whether a numerical imbalance of efferent *vs.* afferent neurons occurred in the adult Bax-KO hippocampus that affected synaptic connectivity. A subset of entorhinal cortex (EC) neurons in layer II project their axons to the outer two-thirds of the molecular layer (OML) of the DG. The gross morphology of the ECappeared normal and was indistinguishable between 2–12 month old WT *vs.* Bax-KO mice (Fig. 2A, B). We next asked whether the dendritic area of DG neurons is modified by the presence of increased cell numbers in the Bax-KO by comparing the thickness of the GCL, OML and the inner molecular layer (IML) of the DG (Fig. 2C, D). The IML was visualized by calretinin labeling, which specifically recognizes the presynaptic nerve terminals of the contralateral hilar neurons in the IML (Liu et al., 1996; Fujise et al., 1998). Although there was a considerable increase in the thickness of GCL in 6 month-old Bax-KO mice, the OML and IML appeared to be normal, suggesting that there is not a proportional increase in synaptic density in response to the increase in DG cell number. Consistent with this, electron microscopic observations of the OML did not reveal any noticeable alterations in the density or morphology of afferent synapses in 2 and 6 month-old Bax-KO mice (Fig. 2E–H). Next, we explored the morphology of dendrites and dendritic spines of DG neurons following Golgi staining. The mean density of dendritic spines in WT and Bax-KO DG neurons was similar (Fig. 2I–K), and there was no significance difference in the frequency distribution of spine density per neuron between the two groups (Fig. 2K, χ^2=26.1, df=18, p=0.098). However, we observed a slight increase in the frequency of DG neurons with thin dendrites

and fewer spines in Bax-KO mice (Fig. 2K, shaded area), which is likely due to the excess numbers of immature neurons and/or compensatory adjustment of synaptic number in Bax-KO mice. Interestingly, we observed that dendritic branch number was reduced in Bax-KO DG neurons compared to WT littermates, based on a Chi-square analysis (Fig. 2L-N, χ^2=18.9, df=6, p=0.004). Collectively, these results suggest that the number of afferent synaptic inputs to each Bax-KO DG neuron is diminished due to a compensatory reduction of dendritic arborization and/or synaptic compensation in the face of the relatively constant amount of innervation from the EC compared to the increased numbers of DG neurons.

Next, we examined the morphology of DG efferent synapses in Bax-KO mice. Mossy fiber (MF) axons were revealed by Timm's staining and the volume of MF axons in WT and Bax-KO mice was measured. Compared to WT littermates and 2-month old Bax-KO mice, the overall volumes of Timm's-stained MF axons and the GCL of the DG were proportionally increased in 6-month old Bax-KO mice, suggesting that most DG neurons, including Bax-KO-rescued neurons, may project MF axons (Fig. 3A, n=4, MF: $F_{(3,12)}$=19.26, P=0.00007, GCL: $F_{(3,12)}$=22.93, P=0.00003). Ultrastructural analyses revealed several alterations in the MF synapses of 6-month old Bax-KO mice. Compared to WT littermates and 2-month old Bax-KO mice (Fig. 3C–D, n=5 in WT; n=4 in 2-month old Bax-KO), the cross-sectional area of MF boutons was greatly reduced (Fig. 3H, $t_{(7)}$=2.59, p=0.004), whereas the area density of MF boutons was increased in 6-month old Bax-KO mice (Fig. 3D). However, there appeared to be similar numbers of CA3 spines in WT and 6-month old Bax-KO mice (Fig. 3D, n=4 in WT; n=5 in KO), and quantification of MFs and CA3 spines confirmed this observation (Fig. 3D). Thus, the ratio of MF:CA3 spines was significantly reduced in 6-month old Bax-KO mice (mean±SEM: WT, 3.5±0.19; Bax-KO, 1.84±0.11, $t_{(7)}$=8.14, p<0.00001). In a frequency-fractionation analysis, the synaptic ratio in WT mice exhibited peaks at fractions 1:3 and 1:4, whereas in 6-month old Bax-KO mice the synaptic ratios were 1:1 (Fig. 3F, χ^2=190.52, df=47, p<0.0001). By contrast, MF synapses of 2-month old Bax-KO mice appeared normal (Fig. 3B, C, E, G), and the apparent slight reduction in synaptic ratio at this age did not reach a statistically significant value (Fig. 3E, χ^2=16.81, df=12, p=0.157).

In summary, it appears that there are adaptive readjustments of the innervation and/or synaptic ratio in the afferent and efferent Bax-KO DG circuits, owing to the progressive accumulation of DG neurons that would have been normally eliminated by Bax-dependent PCD.

Impairment of synaptic efficacy of DG related circuits in 6-month old Bax-KO mice

To assess whether inhibition of PCD influences the synaptic properties of DG connections, we examined the electrophysiological characteristics of both the afferent (mPP) and efferent (MF) pathways to the DG in brain slices. First, we examined the electrophysiological properties of the afferent mPP circuit in the absence or presence of a gamma-aminobutyric acid (GABA) inhibitor, picrotoxin (50 μM). Because mature DG neurons are strongly inhibited by GABA in the mPP pathway, mature neurons contribute little to LTP induction in artificial cerebrospinal fluid (ASCF) (Snyder et al., 2001). Therefore, the small LTP induction in the ACSF condition is mainly attributable to immature neurons which lack GABAergic inhibition. However, picrotoxin treatment can induce strong LTP which is primarily mediated by mature DG neurons. Neither the absence nor presence of picrotoxin resulted in significant modifications of the input-output (I-O) relationships (data not shown) in either 2-month or 6-month old Bax-KO mice compared to WT littermates, suggesting that basic neurotransmission is not affected in Bax-KO mice. In addition, low but substantial LTP induction was similarly observed in both 2-month and 6-month Bax-KO mice in the absence of picrotoxin (Fig. 4A, B). In the presence of picrotoxin, however, 6-month-old Bax-KO mice did not exhibit picrotoxin-promoted LTP induction (Fig. 4D, n=6, 8 slices in

WT; n=11, 18 slices in KO; $t_{(24)}$=2.915, p=0.0076), whereas 2-month old WT and Bax-KO and 6-month old WT mice exhibited marked picrotoxin LTP induction (Fig. 4C, up to 180%). Because picrotoxin-promoted LTP induction is mediated by mature DG neurons, these data indicate that mature DG circuits are impaired in 6-month old Bax-KO mice, whereas immature DG circuits maintain normal electrophysiological properties. Because other circuits such as the lateral perforant-CA3 and Schaffer collateral pathways in 6-month old Bax-KO hippocampal slices appeared virtually normal (Supplementary materials, Fig. S1), it seems likely that circuit modification is related to the age-dependent accumulation of DG neurons in Bax-KO mice.

In the MF circuit analysis, 6-month old Bax-KO mice exhibited a significantly diminished amplitude of the field excitatory postsynaptic potential (fEPSP) responses in an I-O relationship analyses, compared to WT (Fig. 5B, n=5, 5 slices in WT; n=6, 7 slices in KO), whereas 2-month old Bax-KO mice exhibited normal I-O responses (Fig. 5A, n=6, 6 slices in WT; n=5, 5 slices in KO). Furthermore, there was an apparent age-dependent impairment of presynaptic plasticity in Bax-KO mice. We examined paired pulse facilitation (PPF), which occurs when two stimuli are delivered to synapses in rapid succession, resulting in facilitation of the synaptic responses to the second stimulus. Because PPF is a measure of presynaptic function and short-term plasticity (Hessler et al., 1993), we used this to evaluate the presynaptic level of short-term plasticity in Bax-KO mice. Slices from 2-month old WT and Bax-KO mice exhibited similar facilitation at intervals from 40 to 240 msec (Fig. 5C, n=6, 8 slices in WT; n=6, 8 slices in KO), whereas 6-month old Bax-KO mice exhibited significantly less PPF than WT littermates at all intervals (Fig. 5D, n=5, 6 slices in WT; n=8, 11 slices in KO); PPF responses of 6 month-old Bax-KO mice were significantly decreased compared to both 6-month WT and 2-month old mice through all intervals using ANOVA with Shaffe's multiple comparison (40 msec: $F_{(3,29)}$=10.85, P=0.009; 80 msec: $F_{(3,29)}$=8.52, P=0.015; 120 msec: $F_{(3,29)}$=10.61, P=0.011; 240 msec: $F_{(3,29)}$=10.69, P=0.003). We also observed a reduced induction of long-term potentiation (LTP) in 6-month old Bax-KO mice. Following a high frequency stimulus (HFS, 4-trains of 100 Hz for 1 sec with 30 sec intervals) hippocampal slices from 6-month old Bax-KO mice exhibited greatly reduced LTP responses compared to WT (Fig. 5F, n=5, 8 slices in WT; n=8, 8 slices in KO; $t_{(14)}$=4.378, p=0.001). However, in 2-month old Bax-KO hippocampal slices, we obtained LTP responses that were similar to WT littermates (Fig. 5E, n=6, 7 slices in WT; n=7, 9 slices in KO).

Reduced contextual fear learning in Bax-KO mice

We next asked whether the 6-month old Bax-KO mice also exhibited cognitive deficits in addition to the histological and electrophysiological impairment of DG circuits. In a behavioral screening of basic sensory, motor, and cognitive tasks, 6-month old Bax-KO mice exhibited normal sensory and motor functions in the visual cliff test, odor sensitivity test, rotarod test, and pre-pulse inhibition (own unpublished data). We have also examined the spatial learning ability of 6-month old Bax-KO mice using a radial arm maze, and we observed that 6-month old Bax-KO mice and WT littermates exhibited a similar ability to learn, suggesting that normal spatial memory is preserved in the absence of PCD (Supplementary data, Fig. S2C). In addition, object recognition, which is also considered to be hippocampus-dependent (Broadbent et al., 2004), was normal in the 6-month old Bax-KO (Supplementary data, Fig. S2C). Taken together, these results indicate that a subset of hippocampus-related explicit memory tasks was unaffected in 6-month old Bax-KO mice despite the histological and electrophysiological modifications described above.

By contrast, we found that fear conditioning was impaired in 6-month old Bax-KO mice. Following 2, 5, or 10 consecutive conditioning trials, 6-month old WT littermates exhibited a strong freezing response (80% of sessions) in the 2 hr-retention test for contextual fear

memory. However, 6-month old Bax-KO mice exhibited significantly reduced freezing responses following 2-parings for conditioning, although 5- or 10-parings yielded a similar level of freezing behavior in 6-month old WT and Bax-KO mice, suggesting that more extensive repetition of conditioning is required for efficient memory retention in 6-month old Bax-KO mice (Fig. 6A left graph, 2-paired: $t_{(12)}$=7.082, p=0.00001, 5-paired: $t_{(15)}$=0.77, p=0.45, 10-paired: $t_{(10)}$=0.658, p=0.526). In a 24 hr-retention test, the freezing rate of 6-month old Bax-KO mice was also significantly reduced compared to WT littermates in the 2- and 5-parings groups. However 6-month old WT and Bax-KO mice exhibited a similar degree of freezing responses following 10-parings (Fig. 6A right graph, 2-paired: $t_{(12)}$=6.273, p=0.00004, 5-paired: $t_{(15)}$=4.175, p=0.032, 10-paired: $t_{(10)}$=0.896, p=0.391). It is unlikely that reduced fear conditioning performance in 6-month old Bax-KO mice is related to alterations in other aspects of hippocampal-related behaviors such as hyperactivity, because we observed that 5–14-month old Bax-KO mice exhibited a marked impairment in a passive avoidance test which measures associative learning that is relatively unaffected by hyperactivity (Supplementary Fig. S2A).

Interestingly, when the tone (CS) was presented in either the new (cued test) or conditioned (cued+context test) chamber, 6-month old Bax-KO mice exhibited a normal amount of freezing responses (Fig. 6B), suggesting that amygdala-dependent fear memory remains intact in the absence of PCD and that intact cued memory formation in Bax-KO mice can over-ride the deficits in context memory retention. In addition, because there was no difference in the 2-hr and 24-hr retention test for contextual fear memory following 5-parings in 2-month old Bax-KO vs. WT mice, the impairment of fear memory retention in Bax-KO mice is age- and hippocampus-dependent (Fig. 6C), and thus likely related to the selective increased accumulation of Bax-KO rescued neurons in 6-month old animals.

Discussion

Several lines of evidence have suggested the importance of PCD during adult hippocampal neurogenesis. For instance, we observed a relatively low amount of PCD in the developing mouse DG, which is in consistent with reports from the rat (Janowsky & Finlay, 1983; Ferrer et al., 1990). Although other studies report a more substantial PCD of developing DG neurons in the rat (Gould et al., 1991), these discrepancies are likely to be attributable to the species used (mouse *vs.* rat) and/or experimental methods for detecting PCD (pyknosis *vs.* caspase-3). By contrast, a substantially large number (30–70% loss) of newly produced neurons undergo PCD in the adult DG under the standard laboratory housing conditions used here (Cameron & McKay, 2001; Dayer et al., 2003; Sun et al., 2004). Therefore, it has been reported that the developmentally produced neurons numerically dominate the DG population in adulthood (Lagace et al., 2007; Muramatsu et al., 2007; Ninkovic et al., 2007; Imayoshi et al., 2008). Furthermore, the extent of PCD following adult neurogenesis appears to be regulated by neuronal activity/experience. Hippocampal learning, environmental enrichment, or LTP all substantially reduce the PCD of newly produced neurons (Kempermann et al., 1997; Gould et al., 1999; Bruel-Jungerman et al., 2006). Conversely, environmental deprivation or stress enhances the extent of PCD, suggesting that the regulation of PCD is an essential means for regulating the final number of adult produced neurons. In this study, we found that the prevention of PCD in the adult DG leads to compensatory readjustments of synaptic connections, which impair electrophysiological and behavioral aspects of hippocampal function, providing direct evidence that the elimination of neurons is necessary for the maintenance of optimal neuronal function in the adult brain (Fig. 7). Based on our observations, we propose that the elimination of excess neurons by PCD in the adult brain is necessary for optimal systems-matching of mature hippocampal circuits. Our current results also caution that therapeutic over-production or introduction of new neurons in the adult brain may not always produce beneficial effects on brain function.

Impairment of DG related circuits in the absence of PCD in the adult brain

We found that the increase in the number of DG neurons following the prevention of PCD (Sun et al., 2004) is associated with corresponding alterations of synaptic or innervation ratios. For instance, the volume of the MF layer was proportionally increased as a function of the volume of the DG layer, and the area density of MF presynaptic terminals was also increased. However, the area density of CA3 postsynaptic spines was not proportionally increased in 6-month old Bax-KO mice, and the MF:CA3 contact ratio was accordingly reduced. Considering that 2-month old Bax-KO mice have a substantially higher MF:CA3 ratio compared to 6-month old Bax-KO mice, it appears that the reorganization of the synaptic ratio is related to the increased number of Bax-KO DG neurons. However, because our experimental approach did not quantify the absolute number of synapses, we cannot completely rule out the possibility that the alteration of synaptic ratio may be independent of the actual increase in the number of presynaptic boutons. A reorganization of synaptic partnership in the afferent mPP was also observed in the Bax-KO mice, suggesting that both efferent and afferent DG circuits were modified in response to the age-dependent increase in DG neuronal numbers.

An important issue related to these observations is whether the synaptic impairment following the elimination of PCD of newly produced neurons is related to the function of newly produced immature circuits or by the impairment of already established, mature synaptic circuits. This issue was addressed using electrophysiological criteria since it is known that newly generated DG neurons are more efficient in LTP (Wang et al., 2000; Snyder et al., 2001) and that immature DG neurons lack GABAergic inhibition, whereas mature DG neurons are strongly inhibited by GABA (Snyder et al., 2001; Esposito et al., 2005; Tozuka et al., 2005; Tashiro et al., 2006). Therefore, mPP LTP induction in hippocampal slices in the ACSF condition is mainly mediated by immature neuronal circuits, whereas picrotoxin promotes robust LTP induction mediated by mature neuronal circuits. We found that 6-month old Bax-KO mice exhibited an impairment of mPP LTP induction following picrotoxin treatment, whereas this difference was not seen in the ASCF condition, indicating that the impairment observed in the Bax-KO mPP-DG circuit is mainly attributable to an impairment of mature DG neurons *vs.* the accumulation of immature neurons. We previously observed that mature Bax-KO DG neurons progressively reduce their calbindin (CB) expression (Sun et al., 2004). Because the expression of CB is regulated by perturbations of neuronal activity such as seizures and epilepsy (Hwang et al., 2004), these results are consistent with our observation that mature DG neuronal activity is impaired in 6-month old Bax-KO mice. Furthermore, because CB regulates neuronal plasticity via the modulation of peak levels and duration of activity-dependent calcium increases (Baimbridge et al., 1992; Chard et al., 1995), the reduction of CB expression in Bax-KO DG neurons may also affect the efficacy and plasticity of DG circuits. Because surviving adult-produced neurons that are older than 3–4 weeks also contribute to mature DG circuits, we reasoned that the involvement of differentiation-defective, adult-produced neurons may cause the functional impairment of mature DG circuits. On the other hand, Bax-KO mice did not exhibit altered mPP LTP induction in the ACSF condition, suggesting that immature DG neuronal circuits are relatively intact. Considering that Bax-KO mice have substantially increased numbers of immature DG neurons compared to WT littermates (Sun et al., 2004), there are likely compensatory mechanisms that regulate the function of immature DG neurons, and we are currently exploring this issue.

We also found a severe impairment of MF synaptic transmission in Bax-KO mice. In the 6-month old Bax-KO MF, the reduced slope of the I-O curve suggests that the same electrical input to Bax-KO MF may produce a smaller output compared to WT littermates. The reduced MF *vs.* CA3 spine contact numbers appears to influence MF synaptic efficacy, in that the stimulation of a given number of presynaptic fibers may result in a reduction of

postsynaptic CA3 neuronal responses in 6-month old Bax-KO mice (Figure 7). In addition, we found that 6-month old Bax-KO mice exhibited significantly reduced short-term presynaptic plasticity and a greatly reduced ability to produce MF LTP. Because MF LTP is largely mediated by a presynaptic mechanism (Nicoll and Malenka, 1995), reduced synaptic transmission efficacy and reduced presynaptic plasticity appear to contribute to the impairment of MF LTP induction. In contrast to the marked impairment of 6-month old Bax-KO DG circuits, 2-month old DG circuits and 6-month old lateral perforant pathway-CA3 circuits and Schaffer/Collateral pathways were all spared in Bax-KO mice. This indicates that neither cell-autonomous alterations owing to the absence of Bax protein nor changes in developmental events (e.g. developmental PCD of neurons) appear to be critically involved in the impairment of the DG connections we observed.

Bax-KO mice exhibit a subset of normal hippocampus-dependent behaviors

Our results demonstrate that the prevention of PCD results in the reduced efficacy of a subset of hippocampus-related memory acquisition and consolidation events, suggesting that PCD in the adult brain may be required for the maintenance of efficient memory processes. Supporting our observation, it has also been reported that transgenic mice overexpressing Bcl-2 in the nervous system exhibited deficits in fear-related allocentric navigation ability as well as an apparent increase in DG cell number (Rondi-Reig et al., 2001; Kuhn et al., 2005). Adult neurogenesis has been proposed as a means to enhance the behavioral adaptability of animals (Cecchi et al., 2001). Supporting this idea, it has recently been demonstrated that the prevention of DG neurogenesis impairs contextual fear conditioning (Saxe et al., 2006), which is similar to our results following the suppression of PCD in Bax-KO mice. However, these two conditions impair different DG circuits (i.e. the impairment of immature circuits after the prevention of neurogenesis *vs.* the impairment of mature circuits after the prevention of PCD), and together these results suggest that both immature and mature DG neurons are normally required for contextual fear conditioning. Alternatively, it is also possible that an optimal number of DG neurons, regardless of their birthdates may be important for normal function in the hippocampus.

In contrast to the substantial impairment of fear conditioning behavior, other hippocampus-related behaviors such as spatial learning and novel object recognition, were relatively spared in Bax-KO mice. Similar to the Bax-KO mice, the conditional knock-out of the N-methyl-D-aspartate, NMDA receptor subunits in CA3 or DG neurons fails to modify basal spatial learning ability in a water-maze paradigm (Nakazawa et al., 2002; McHugh et al., 2007), suggesting that the DG circuits may be less closely related to spatial learning. Neurogenesis is apparently not affected by the performance of specific spatial learning tasks in the rat (van Praag et al., 1999; Merrill et al., 2003), and suppression of hippocampal neurogenesis does not alter spatial memory (Saxe et al., 2006). However, the suppression of adult hippocampal neurogenesis modifies spatial working memory (Saxe et al., 2006), indicating that neurogenesis and likely PCD as well may impact rather specific aspects of spatial learning ability (Rondi-Reig et al., 2001). Recently, it has been reported that treatment with a caspase inhibitor to reduce PCD in the adult brain perturbed spatial learning in the rat (Dupret et al., 2007). Because the transient blockade of PCD by caspase inhibition may primarily impact immature DG circuits (Dupret et al., 2007), this observation supports the idea that the Bax-KO phenotype observed in the current study may reflect the role of mature DG circuits. Alternatively, it is possible that the results from Dupret et al are related to the reported apoptosis-independent function of caspases on synapses and synaptic plasticity (Gulyaeva et al., 2003; Lu et al., 2006). However, we also cannot completely exclude the possibility that the modification of PCD in other brain circuits in Bax-KO mice may compensate for a loss of DG-mediated spatial learning ability.

An indispensable role for PCD in the elimination of excess connections in the adult brain

Competition among embryonic neurons is a mechanism regulating the initial formation and quantitative refinement of neuronal connections during development (the neurotrophic hypothesis) (Kintner, 2002). Recent evidence indicates that competition among adult produced neurons is also crucial for their survival (Tashiro et al., 2006), suggesting that PCD of adult produced neurons may recapitulate the developmental process of systems-matching. Compared to the embryonic situation, however, mature neurons in the adult brain comprise the major neuronal circuits and thus adult-generated immature neurons may compete with these mature neurons for survival and/or synaptic contacts. During competition among neurons that are at different stages of differentiation, it appears that adult-produced immature DG neurons are able to innervate CA3 dendritic spines which would have originally made MF synapses with mature DG neurons. For example, it has been recently demonstrated that the dendritic spines on newborn DG neurons are capable of making contact with pre-existing presynaptic boutons (Toni et al., 2007). Therefore, there may be a competition/interaction between mature *vs.* immature neurons for establishing synaptic contacts, and the survival of excess DG neurons in Bax-KO mice may perturb this competition. In this respect, our present results are in sharp contrast to the phenotype observed in some other neuronal populations which are rescued from developmental PCD in Bax-KO mice. Previously we demonstrated that most excess motoneurons rescued from PCD in Bax-KO mice are not able to maintain neuromuscular connections and thus are excluded from functional neural circuits (Sun et al., 2003). Therefore, Bax-KO mice exhibit relatively normal neuromuscular function (Buss et al., 2006b; Buss et al., 2006a), suggesting that in this case elimination or prevention of excess synaptic connections from rescued neurons may compensate for increased neuronal survival in the absence of PCD. However, as shown here excess adult produced DG neurons in Bax-KO mice appear to form and maintain synaptic connections. In this respect, PCD of adult-generated neurons in the brain may be more indispensable for systems-matching than PCD occurring during early development.

Supplementary Material

Refer to Web version on PubMed Central for supplementary material.

Acknowledgments

We especially thank Dr. Jung, MW at Ajou University for his comments. Supported by the Korean Ministry of Science and Technology grants (to WS, M10412000078-04N1200-07810), 21C Frontier Brain Research Center (to HK, M103KV010018-03K2201-01820), KOSEF (to SWC, R01-2004-000-10613-0) and by NIH grants NS20402 and NS048982 (RWO).

Abbreviations

DG	dentate gyrus
PCD	programmed cell death
MF	mossy fiber
BrdU	bromodeoxyuridine
WT	wildtype
Bax-KO	Bax-deficient
ASCF	artificial cerebrospinal fluid
fEPSP	field excitatory postsynaptic potential

LTP	long term potentiation
PPF	post synaptic facilitation
mPP	medial perforant pathway
GCL	granule cell layer
CS	conditioned stimuli
US	unconditioned stimuli
EC	enthorhinal cortex
OML	outer molecular layer
IML	inner molecular layer
GABA	γ-aminobutyric acid
HFS	high frequency stimulation
CB	calbindin

References

Altman J, Das GD. Autoradiographic and histological evidence of postnatal hippocampal neurogenesis in rats. J Comp Neurol. 1965; 124:319–335. [PubMed: 5861717]

Baimbridge KG, Celio MR, Rogers JH. Calcium-binding proteins in the nervous system. Trends Neurosci. 1992; 15:303–308. [PubMed: 1384200]

Ben Abdallah NM, Slomianka L, Vyssotski AL, Lipp HP. Early age-related changes in adult hippocampal neurogenesis in C57 mice. Neurobiol Aging. 2008 In press.

Broadbent NJ, Squire LR, Clark RE. Spatial memory, recognition memory, and the hippocampus. Proc Natl Acad Sci U S A. 2004; 101:14515–14520. [PubMed: 15452348]

Bruel-Jungerman E, Davis S, Rampon C, Laroche S. Long-term potentiation enhances neurogenesis in the adult dentate gyrus. J Neurosci. 2006; 26:5888–5893. [PubMed: 16738230]

Buss RR, Sun W, Oppenheim RW. Adaptive roles of programmed cell death during nervous system development. Ann Rev Neurosci. 2006a; 29:1–35. [PubMed: 16776578]

Buss RR, Gould TW, Ma J, Vinsant S, Prevette D, Winseck A, Toops KA, Hammarback JA, Smith TL, Oppenheim RW. Neuromuscular development in the absence of programmed cell death: phenotypic alteration of motoneurons and muscle. J Neurosci. 2006b; 26:13413–13427. [PubMed: 17192424]

Cameron HA, McKay RD. Adult neurogenesis produces a large pool of new granule cells in the dentate gyrus. J Comp Neurol. 2001; 435:406–417. [PubMed: 11406822]

Cao L, Jiao X, Zuzga DS, Liu Y, Fong DM, Young D, During MJ. VEGF links hippocampal activity with neurogenesis, learning and memory. Nat Genet. 2004; 36:827–835. [PubMed: 15258583]

Caviness VS Jr. Time of neuron origin in the hippocampus and dentate gyrus of normal and reeler mutant mice: an autoradiographic analysis. J Comp Neurol. 1973; 151:113–120. [PubMed: 4744470]

Cecchi GA, Petreanu LT, Alvarez-Buylla A, Magnasco MO. Unsupervised learning and adaptation in a model of adult neurogenesis. J Comput Neurosci. 2001; 11:175–182. [PubMed: 11717533]

Chard PS, Jordan J, Marcuccilli CJ, Miller RJ, Leiden JM, Roos RP, Ghadge GD. Regulation of excitatory transmission at hippocampal synapses by calbindin D28k. Proc Natl Acad Sci U S A. 1995; 92:5144–5148. [PubMed: 7761464]

Dayer AG, Ford AA, Cleaver KM, Yassaee M, Cameron HA. Short-term and long-term survival of new neurons in the rat dentate gyrus. J Comp Neurol. 2003; 460:563–572. [PubMed: 12717714]

Debiec J, Doyère V, Nader K, LeDoux LE. Directly reactivated, but not indirectly reactivated, memories undergo reconsolidation in the amygdala. Proc Natl Adad Sci U S A. 2006; 103:3428–3433.

Denis-Donini S, Dellarole A, Crociara P, Francese MT, Bortolotto V, Quadrato G, Canonico PL, Orsetti M, Ghi P, Memo M, Bonini SA, Ferrari-Toninelli G, Grilli M. Impaired adult neurogenesis associated with short-term memory defects in NF-kappaB p50-deficient mice. J Neurosci. 2008; 28:3911–3919. [PubMed: 18400889]

Doyère V, Dębiec J, Monfils MH, Schafe GE, LeDoux JE. Synapse-specific reconsolidation of distinct fear memories in the lateral amygdala. Nature Neurosci. 2007; 10:414–416. [PubMed: 17351634]

Dupret D, Fabre A, Dobrossy MD, Panatier A, Rodriguez JJ, Lamarque S, Lemaire V, Oliet SH, Piazza PV, Abrous DN. Spatial learning depends on both the addition and removal of new hippocampal neurons. PLoS Biol. 2007; 5:e214. [PubMed: 17683201]

Eriksson PS, Perfilieva E, Bjork-Eriksson T, Alborn AM, Nordborg C, Peterson DA, Gage FH. Neurogenesis in the adult human hippocampus. Nat Med. 1998; 4:1313–1317. [PubMed: 9809557]

Esposito MS, Piatti VC, Laplagne DA, Morgenstern NA, Ferrari CC, Pitossi FJ, Schinder AF. Neuronal differentiation in the adult hippocampus recapitulates embryonic development. J Neurosci. 2005; 25:10074–10086. [PubMed: 16267214]

Feng R, Rampon C, Tang YP, Shrom D, Jin J, Kyin M, Sopher B, Miller MW, Ware CB, Martin GM, Kim SH, Langdon RB, Sisodia SS, Tsien JZ. Deficient neurogenesis in forebrain-specific presenilin-1 knockout mice is associated with reduced clearance of hippocampal memory traces. Neuron. 2001; 32:911–926. [PubMed: 11738035]

Ferrer I, Serrano T, Soriano E. Naturally occurring cell death in the subicular complex and hippocampus in the rat during development. Neurosci Res. 1990; 8:60–66. [PubMed: 2163051]

Fujise N, Liu Y, Hori N, Kosaka T. Distribution of calretinin immunoreactivity in the mouse dentate gyrus: II. Mossy cells, with special reference to their dorsoventral difference in calretinin immunoreactivity. Neuroscience. 1998; 82:181–200. [PubMed: 9483514]

Gould E, Woolley CS, McEwen BS. Naturally occurring cell death in the developing dentate gyrus of the rat. J Comp Neurol. 1991; 304:408–418. [PubMed: 2022756]

Gould E, Beylin A, Tanapat P, Reeves A, Shors TJ. Learning enhances adult neurogenesis in the hippocampal formation. Nat Neurosci. 1999; 2:260–265. [PubMed: 10195219]

Greenough WT, Cohen NJ, Juraska JM. New neurons in old brains: learning to survive? Nat Neurosci. 1999; 2:203–205. [PubMed: 10195209]

Gross CG. Neurogenesis in the adult brain: death of a dogma. Nat Rev Neurosci. 2000; 1:67–73. [PubMed: 11252770]

Gulyaeva NV, Kudryashov IE, Kudryashova IV. Caspase activity is essential for long-term potentiation. J Neurosci Res. 2003; 73:853–864. [PubMed: 12949912]

Hamburger V, Oppenheim RW. Naturally occurring neuronal death in vertebrates. Neurosci Comm. 1982; 1:39–55.

Hessler NA, Shirke AM, Malinow R. The probability of transmitter release at a mammalian central synapse. Nature. 1993; 366:569–572. [PubMed: 7902955]

Hwang IK, Lee HY, Seong NS, Chung HG, Kim JH, Lee HJ, Kim JD, Kang TC, Won MH. Changes of calbindin D-28k immunoreactivity in the hippocampus after adrenalectomy in the seizure sensitive gerbil. Anat Histol Embryol. 2004; 33:299–303. [PubMed: 15352884]

Imayoshi I, Sakamoto M, Ohtsuka T, Takao K, Miyakawa T, Yamaguchi M, Mori K, Ikeda T, Itohara S, Kageyama R. Roles of continuous neurogenesis in the structural and function integrity of the adult forebrain. Nat Neurosci. 2008; 11:1153–1161. [PubMed: 18758458]

Janowsky JS, Finlay BL. Cell degeneration in early development of the forebrain and cerebellum. Anat Embryol (Berl). 1983; 167:439–447. [PubMed: 6625197]

Kaplan MS, Hinds JW. Neurogenesis in the adult rat: electron microscopic analysis of light radioautographs. Science. 1977; 197:1092–1094. [PubMed: 887941]

Kempermann G, Kuhn HG, Gage FH. More hippocampal neurons in adult mice living in an enriched environment. Nature. 1997; 386:493–495. [PubMed: 9087407]

Kintner C. Neurogenesis in embryos and in adult neural stem cells. J Neurosci. 2002; 22:639–643. [PubMed: 11826093]

Knudson CM, Tung KS, Tourtellotte WG, Brown GA, Korsmeyer SJ. Bax-deficient mice with lymphoid hyperplasia and male germ cell death. Science. 1995; 270:96–99. [PubMed: 7569956]

Kuhn HG, Biebl M, Li M, Friedlander RM, Winkler J. Increased generation of granule cells in adult Bcl-2-overexpressing mice: a role for cell death during continued hippocampal neurogenesis. Eur J Neurosci. 2005; 22:1907–1915. [PubMed: 16262630]

Kuhn HG, Dickinson-Anson H, Gage FH. Neurogenesis in the dentate gyrus of the adult rat: age-related decrease of neuronal progenitor proliferation. J Neurosci. 1996; 16:2027–2033. [PubMed: 8604047]

Lagace DC, Whitman MC, Noonan MA, Ables JL, DeCarolis NA, Arguello AA, Donovan MH, Fisher SJ, Farnbauch LA, Beech RD, DiLeone RJ, Greer CA, Mandyam CD, Eisch AJ. Dynamic contribution of nestin-expressing stem cells to adult neurogenesis. J Neurosci. 2007; 27:12623–12629. [PubMed: 18003841]

Leuner B, Mendolia-Loffredo S, Kozorovitskiy Y, Samburg D, Gould E, Shors TJ. Learning enhances the survival of new neurons beyond the time when the hippocampus is required for memory. J Neurosci. 2004; 24:7477–7481. [PubMed: 15329394]

Liu Y, Fujise N, Kosaka T. Distribution of calretinin immunoreactivity in the mouse dentate gyrus. I General description. Exp Brain Res. 1996; 108:389–403. [PubMed: 8801119]

Lu C, Wang Y, Furukawa K, Fu W, Ouyang X, Mattson MP. Evidence that caspase-1 is a negative regulator of AMPA receptor-mediated long-term potentiation at hippocampal synapses. J Neurochem. 2006; 97:1104–1110. [PubMed: 16573645]

McHugh TJ, Jones MW, Quinn JJ, Balthasar N, Coppari R, Elmquist JK, Lowell BB, Fanselow MS, Wilson MA, Tonegawa S. Dentate gyrus NMDA receptors mediate rapid pattern separation in the hippocampal network. Science. 2007; 317:94–99. [PubMed: 17556551]

Merrill DA, Karim R, Darraq M, Chiba AA, Tuszynski MH. Hippocampal cell genesis does not correlate with spatial learning ability in aged rats. J Comp Neurol. 2003; 459:201–207. [PubMed: 12640670]

Muramatsu R, Ikegaya Y, Matsuki N, Koyama R. Neonatally born granule cells numerically dominate adult mice dentate gyrus. Neuroscience. 2007; 148:593–598. [PubMed: 17706367]

Nakazawa K, Quirk MC, Chitwood RA, Watanabe M, Yeckel MF, Sun LD, Kato A, Carr CA, Johnston D, Wilson MA, Tonegawa S. Requirement for hippocampal CA3 NMDA receptors in associative memory recall. Science. 2002; 297:211–218. [PubMed: 12040087]

Nicoll RA, Malenka RC. Contrasting properties of two forms of long-term potentiation in the hippocampus. Nature. 1995; 377:115–118. [PubMed: 7675078]

Ninkovic J, Mori T, Götz M. Distinct modes of neuron addition in adult mouse neurogenesis. J Neurosci. 2007; 27:10906–10911. [PubMed: 17913924]

Oppenheim RW. Cell death during development of the nervous system. Ann Rev Neurosci. 1991; 14:453–501. [PubMed: 2031577]

Purves, D. Body and Brain: A Trophic Theory of Neural Connections. Harvard University Press; Cambridge: 1988.

Ramirez-Amaya V, Balderas I, Sandoval J, Escobar ML, Bermudez-Rattoni F. Spatial long-term memory is related to mossy fiber synaptogenesis. J Neurosci. 2001; 21:7340–7348. [PubMed: 11549744]

Rhyu IJ, Abbott LC, Walker DB, Sotelo C. An ultrastructural study of granule cell/Purkinje cell synapses in tottering (tg/tg), leaner (tg(la)/tg(la)) and compound heterozygous tottering/leaner (tg/tg(la)) mice. Neuroscience. 1999; 90:717–728. [PubMed: 10218773]

Rondi-Reig L, Lemaigre-Dubreuil L, Montécot C, Müller D, Martinou JC, Caston J, Mariani J. Transgenic mice with neuronal overexpression of Bcl-2 gene present navigation disability in a water task. Neuroscience. 2001; 104:207–215. [PubMed: 11311543]

Saxe MD, Battaglia F, Wang JW, Malleret G, David DJ, Monckton JE, Garcia AD, Sofroniew MV, Kandel ER, Santarelli L, Hen R, Drew MR. Ablation of hippocampal neurogenesis impairs contextual fear conditioning and synaptic plasticity in the dentate gyrus. Proc Natl Acad Sci U S A. 2006; 103:17501–17506. [PubMed: 17088541]

Schmitz D, Mellor J, Breustedt J, Nicoll RA. Presynaptic kainate receptors impart an associative property to hippocampal mossy fiber long-term potentiation. Nat Neurosci. 2003; 6:1058–1063. [PubMed: 12947409]

Snyder JS, Kee N, Wojtowicz JM. Effects of adult neurogenesis on synaptic plasticity in the rat dentate gyrus. J Neurophysiol. 2001; 85:2423–2431. [PubMed: 11387388]

Sun W, Gould TW, Vinsant S, Prevette D, Oppenheim RW. Neuromuscular development after the prevention of naturally occurring neuronal death by Bax deletion. J Neurosci. 2003; 23:7298–7310. [PubMed: 12917363]

Sun W, Winseck A, Vinsant S, Park OH, Kim H, Oppenheim RW. Programmed cell death of adult-generated hippocampal neurons is mediated by the proapoptotic gene Bax. J Neurosci. 2004; 24:11205–11213. [PubMed: 15590937]

Tashiro A, Sandler VM, Toni N, Zhao C, Gage FH. NMDA-receptor-mediated, cell-specific integration of new neurons in adult dentate gyrus. Nature. 2006; 442:929–933. [PubMed: 16906136]

Toni N, Teng EM, Bushong EA, Aimone JB, Zhao C, Consiglio A, van Praag H, Martone ME, Ellisman MH, Gage FH. Synapse formation on neurons born in the adult hippocampus. Nat Neurosci. 2007; 10:727–734. [PubMed: 17486101]

Tozuka Y, Fukuda S, Namba T, Seki T, Hisatsune T. GABAergic excitation promotes neuronal differentiation in adult hippocampal progenitor cells. Neuron. 2005; 47:803–815. [PubMed: 16157276]

van Praag H, Christie BR, Sejnowski TJ, Gage FH. Running enhances neurogenesis, learning, and long-term potentiation in mice. Proc Natl Acad Sci U S A. 1999; 96:13427–13431. [PubMed: 10557337]

Wang S, Scott BW, Wojtowicz JM. Heterogenous properties of dentate granule neurons in the adult rat. J Neurobiol. 2000; 42:248–257. [PubMed: 10640331]

Wiskott L, Rasch MJ, Kempermann G. A functional hypothesis for adult hippocampal neurogenesis: avoidance of catastrophic interference in the dentate gyrus. Hippocampus. 2006; 16:329–343. [PubMed: 16435309]

Zhang CL, Zou Y, He W, Gage FH, Evans RM. A role for adult TLX-positive stem cells in learning and behavior. Nature. 2008; 451:1004–1007. [PubMed: 18235445]

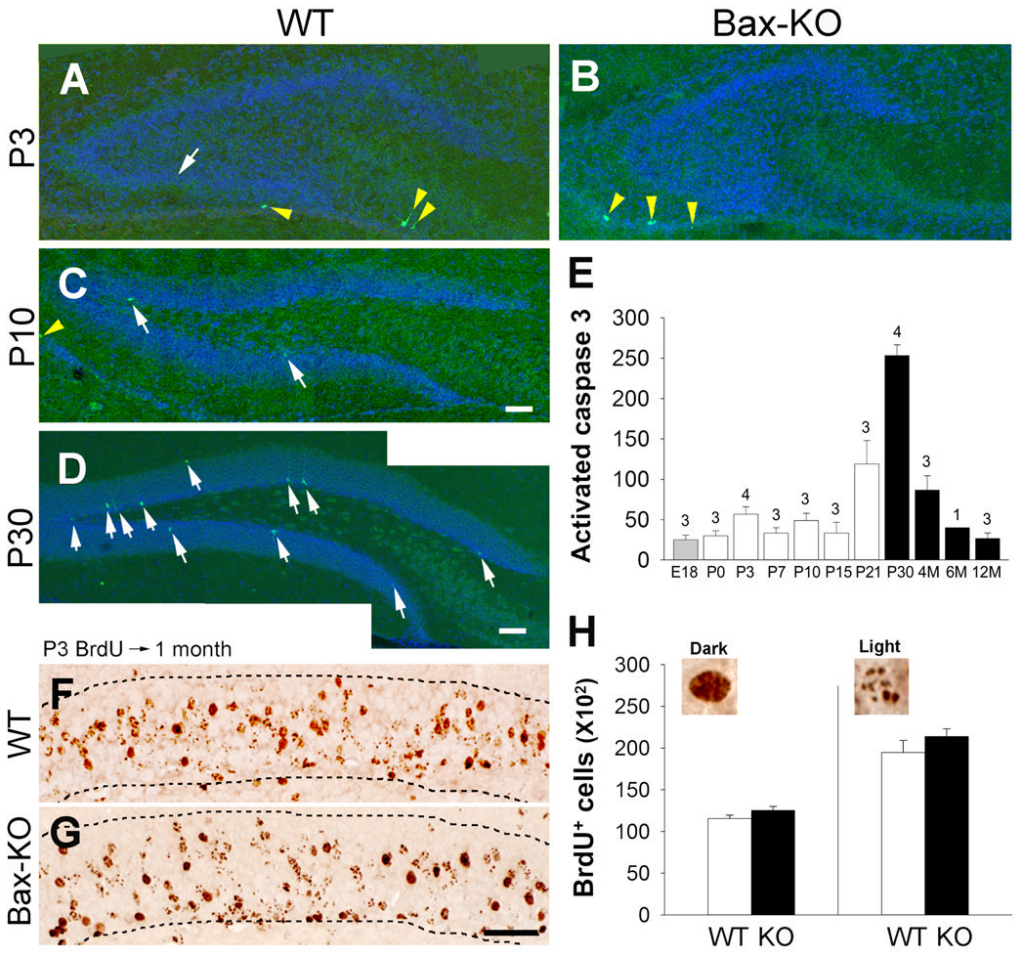

Fig. 1.

The PCD of developmentally produced DG neurons in WT and Bax-KO mice. **A–B**: Activated caspase-3 (green) in P3 (**A, B**), P10 (**C**), and P30 (**D**) WT (**A,C,D**) and Bax-KO (**B**) mice. Nuclei were counter-stained with Hoechst33342 (blue). White arrows indicate activated caspase3-labeled cells in the DG. Yellow arrowheads indicate activated caspase3-labeled cells in the paraventricular region surrounding hippocampal formation. Scale bar=100 μm **E**: Quantification of activated caspase-3-labeled cells in the WT DG. Note that activated caspase3-labeled dying cells are substantially increased after the major developmental neurogenic period (filled bars). Data=mean± s.e.m. The number of animals used in each group is shown over each bar. **F–G**: Survival (1-month) of P3-born BrdU-labeled cells in WT (**F**) and Bax-KO mice (**G**) DG. Animals received BrdU (50 mg/kg) on P3, and total number of BrdU-labeled cells in the DG was assessed 1 month later. Dashed lines indicate the borders of the GCL. Note that many neurons exhibited punctate-like nuclear BrdU-labeling, owing to the dilution of BrdU during additional rounds of cell division. **H**: Quantification of BrdU-labeled cells in the DG. We separately quantified dark-labeled, and punctate/light-labeled BrdU-positive nuclei within the GCL. Typical examples of each category are shown at the top of the graph. Data=mean± s.e.m., n=3.

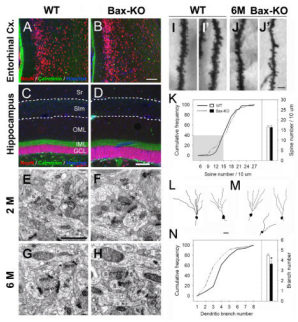

Fig. 2.

Histological analyses of DG afferents and DG neurons in 6-month old mice. **A–B**: Gross morphology of WT (**A**) and the Bax-KO (**B**) entorhinal cortex. NeuN (red) and Calretinin (green, a marker for the subset of interneurons) double labeling to visualize general morphology. Nuclei were counterstained with Hoechst33342 (blue). **C–D**: NeuN- and Calretinin-labeled DG areas in WT (**C)** and Bax-KO (**D**) mice. Periventricular-molecular layer border and stratum lacunosum moleculare (Slm) are marked by dotted lines, respectively. Sr, stratum radiatum; OML, outer molecular layer; IML, inner molecular layer; DG, dentate gyrus. **E–H**: Electron microscopic images of mPP:DG synapses in the 2-month (2 M, **E, F**) and 6-month (6 M, **G, H**) old WT (**E, G**) and Bax-KO (**F, H**) mice. Presynaptic boutons are labeled as mPP, and postsynaptic density (PSD)-containing DG spines are labeled as S. **I-J**: Golgi stained dendritic morphology of WT (**I, I′**), and Bax-KO (**J, J′**) DG neurons. **K:** Cumulative frequency of dendritic spine density per neuron (left) and mean values (right bar graph). A total of 100 neurons from 5 different mice (20 cells/mouse) in each group were included for analyses. The frequency of the Bax-KO DG neurons with thin dendrites and reduced spines (**J′**) is slightly increased (gray shaded area). **L–M**: A camera lucida drawing of dendritic arborization in WT (**L**) and Bax-KO (**M**) DG neurons. **N**: Cumulative frequency of dendritic branch numbers per neuron. A total of 100 neurons from 5 different mice (20 cells/mouse) in each group were included for analyses (*$p<0.05$, t-test). Scale bar= 100 μm in B, D, 1 μm in E, 10 μm in J′, 20 μm in L.

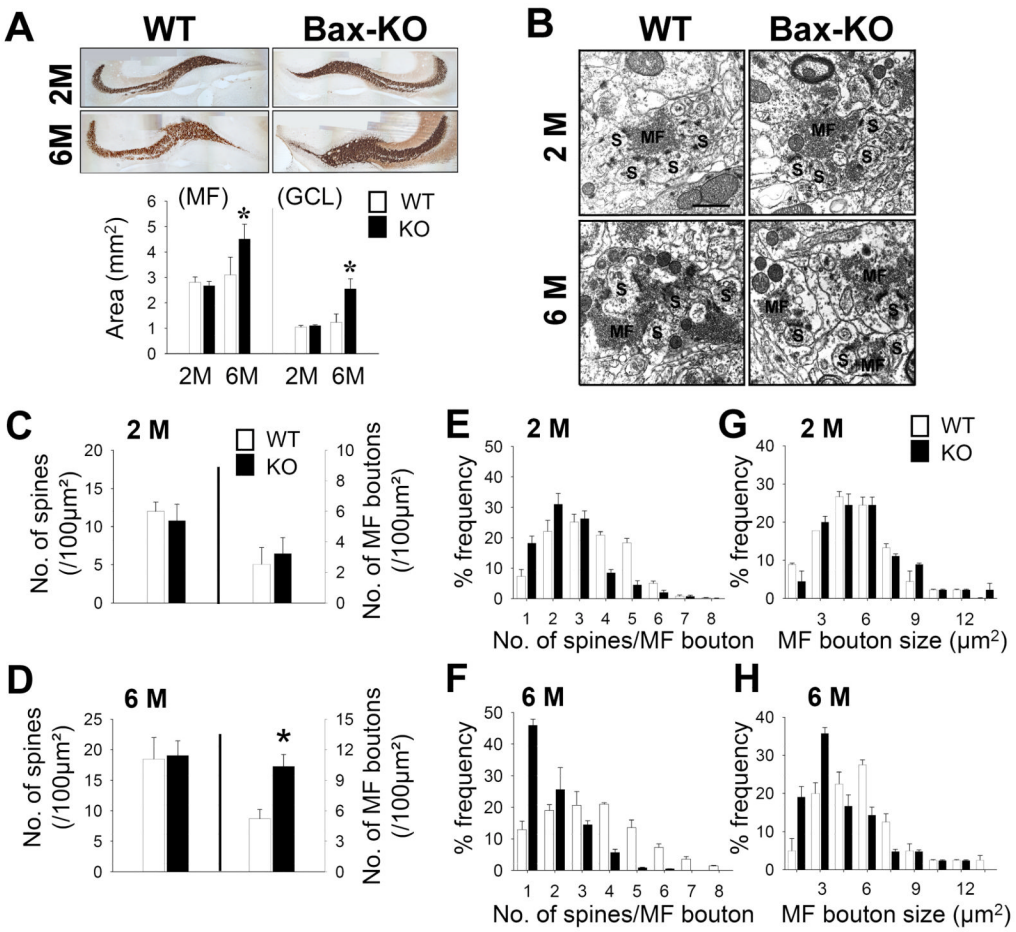

Fig. 3.

Histological analyses of MF connections. **A**: Timm's staining revealed MF labeling in 2-month old and 6-month old WT and Bax-KO mice. Scale bar = 300 μm. Quantification of the MF and granule cell layer of DG areas (n=4, *p<0.05, t-test) is presented in the graph (bottom). **B**: Electron microscopic images of MF:CA3 synapses in 2-month old and 6-month old mice. MF boutons are labeled as MF, and postsynaptic density (PSD)-containing CA3 spines are labeled as S. Scale bar=1 μm. **C–D:** Density of spines and MF boutons in 2-month old (**C**, n=5 in WT, n=4 in KO) and 6-month old (**D**, n=4 in WT, n=5 in KO) groups. MFs contacting dendritic spines containing a PSD were included in the counts (*p<0.05, t-test). **E–H:** Frequency-fractionation analyses of the MF:CA3 ratio in 2-month old (**E**) and 6-month old (**F**) mice. Frequency-fractionation analyses of the size of MF boutons in the 2-month (**G**) and 6-month old groups (**H**). Data are expressed as mean±s.e.m.

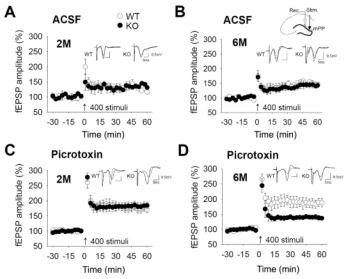

Fig. 4.

Electrophysiological properties of the mPP in Bax-KO hippocampus. **A, B**: Time-course changes in fEPSP amplitude following high-frequency stimulation (4 trains, 100 Hz for 1 sec) in 2-month old (**A**, n=4, 5 slices in WT, n=5, 5 slices in KO), and 6-month old (**B**, n=3, 3 slices in WT, n=3, 3 slices in KO) groups in the ACSF condition. The small diagram in **B** shows the sites of stimulation (black arrow head) and recording (white arrow head). **C, D**: LTP profiles in 2-month old (**C**, n=5, 7 slices in WT, n=8, 11 slices in KO) and 6-month old (**D**, n=6, 8 slices in WT, n=11, 18 slices in KO) groups in the presence of picrotoxin (50 μM), a GABA blocker. Representative recordings at times 0 and 60 min are shown in the inset. All LTP profiles are expressed as mean±s.e.m of average values of a 3-min block.

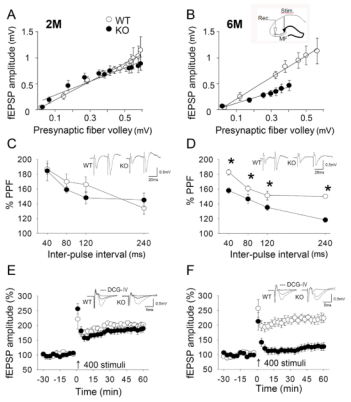

Fig. 5.

Electrophysiological properties of MF in Bax-KO hippocampus. **A, B**: Input-output relationship of the amplitude of fEPSP in 2-month old Bax-KO mice (**A**, n=6, 6 slices in WT, n=5, 5 slices in KO), and in 6-month old Bax-KO mice (**B**, n=5, 5 slices in WT, n=6, 7 slices in KO) followed by gradually increased intensity of the MF stimulus. The small diagram in **B** shows the sites of stimulation (black arrow head) and recording (white arrow head). **C, D**: PPF in 2-month old (**C**, n=6, 8 slices in WT, n=6, 8 slices in KO) and 6-month old (**D**, n=5, 6 slices in WT, n=8, 11 slices in KO) groups. The ordinate indicates the ratio of the second fEPSP amplitude relative to the first one at each inter-pulse interval. A typical field response evoked by paired-pulse stimuli with a 40 msec interval is shown in the inset (*$p<0.05$; two-tailed t-test). **E, F**: Time-course change in fEPSP amplitude following high-frequency stimulation (4-train, 100 Hz for 1 sec) in 2-month old (**E**, n=6, 7 slices in WT, n=7, 9 slices in KO), and 6-month old (**F**, n=5, 8 slices in WT, n=8, 8 slices in KO) groups. Representative recordings at times 0 and 60 min are shown in the inset. All LTP profiles are expressed as mean±s.e.m of average values of a 3-min block.

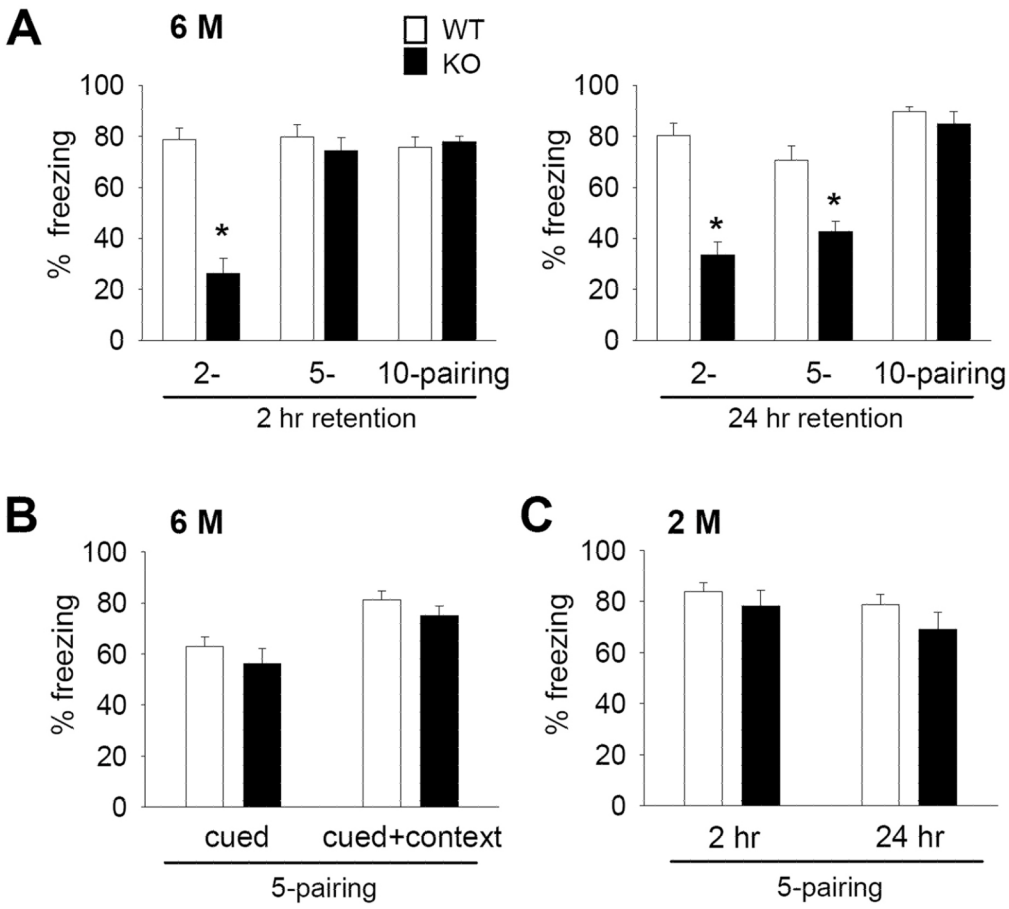

Fig. 6.

Impaired contextual fear memory in 6-month old Bax-KO mice. **A**: Contextual fear memory in 6-month old (6 M) Bax-KO mice. Two-hr (left graph) and 24-hr freezing rate measures (right graph) after 2- (n=8 in WT, n=6 in Bax-KO mice), 5- (n=8 in WT, n=9 in Bax-KO mice) and 10-(n=6 in WT and Bax-KO mice) parings (*p>0.05, two-tailed t-test). **B**: Normal cued fear memory retention in the 6-month old Bax-KO mice. In the 5-paired training groups, cued and cued+context fear retention was determined 3 hrs after the 24-hr context test (n=8 in WT, n=9 in Bax-KO mice, see materials and methods). **C**: Freezing rate in the 2 hr and 24 hr retention tests for contextual fear memory in the 2-month (2 M) old group following 5-pairings (n=6 in WT and Bax-KO mice). Data are expressed as mean± s.e.m.

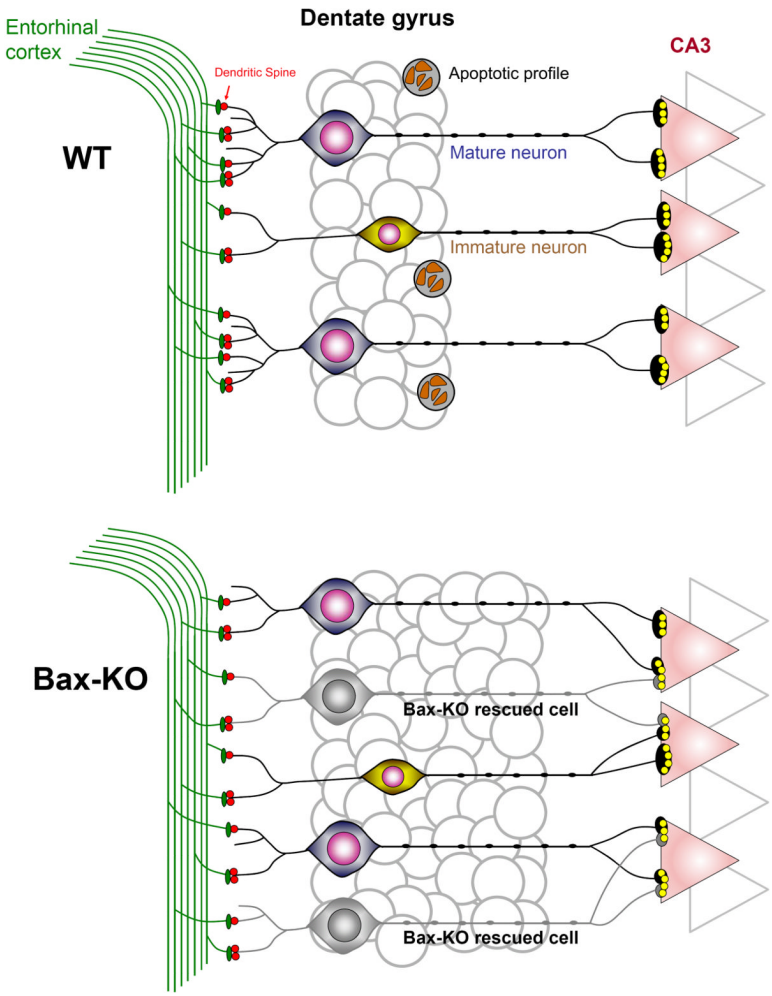

Fig. 7.

Schematic diagram of the readjustment of hippocampal synaptic connections following the prevention of PCD in adult Bax-KO mice. Whereas a subset of adult-produced neurons undergo PCD in WT, all adult-produced neurons in Bax-KO mice survive and compete with mature DG neurons for synaptic contact. In the face of limited afferents, competition among outnumbered DG neurons results in a reduction of dendritic arborization of DG neurons. Similarly, in the face of virtually constant number of CA3 dendritic spines, excess efferent fibers from Bax-KO-rescued DG neurons results in a reduction of the MF:CA3 synaptic ratio. These synaptic readjustments appear to affect neurotransmission and/or synaptic plasticity of efferent/afferent DG circuits and perturb fear conditioning.